Nonlinear Redundancy Analysis of Multi-Cell Pre-stressed Concrete Box-Girder Bridge

Analysis Report

Bala Sivakumar PE
O. Murat Hamutcuoglu Ph.D.
HNTB Corporation

Dr. Michel Ghosn Ph.D.
The City College of New York / CUNY

JUNE 2013

NON-LINEAR ANALYSIS OF PRE-STRESSED CONCRETE BOX-GIRDER BRIDGE

This document describes the model and covers the details of the analysis setup for a multi-cell pre-stressed concrete box- girder bridge example. The original bridge model was set up by CALTRANS to perform a pushover analysis for the seismic design of the bridge using SAP2000 commercial software. The original model represents the pre-stressed concrete multi- cell box-girder superstructure using elastic shell elements as illustrated in Figure 1. The column and the integral cap beam at the piers are modeled using beam- column type finite elements. The original model is well detailed to represent the inelastic pier behavior directly for pushover analysis under the effect of a lateral load. However, the superstructure model with elastic shell elements is not sufficient to represent the inelastic interaction between the concrete, reinforcing steel, and pre-stressing tendons and it cannot be used for a "pushdown" analysis that studies the nonlinear behavior of the structure under increasing vertical loads. For this reason, a second model is created where the inelastic section behavior of the box girders is incorporated. The analysis setup is prepared in SAP2000 v15 Advanced providing complex analysis features including non-linear pushover and pushdown analyses. In this Report, the original model with an integral connection between the cap beam and the columns will be identified as Model 1. A modified model where the columns are assumed to be connected to the cap beam by bearings will be identified as Model 2. A more advanced space frame model that considers the nonlinear behavior of the superstructure will be identified as Model 3. The details of the setup and the models are given below.

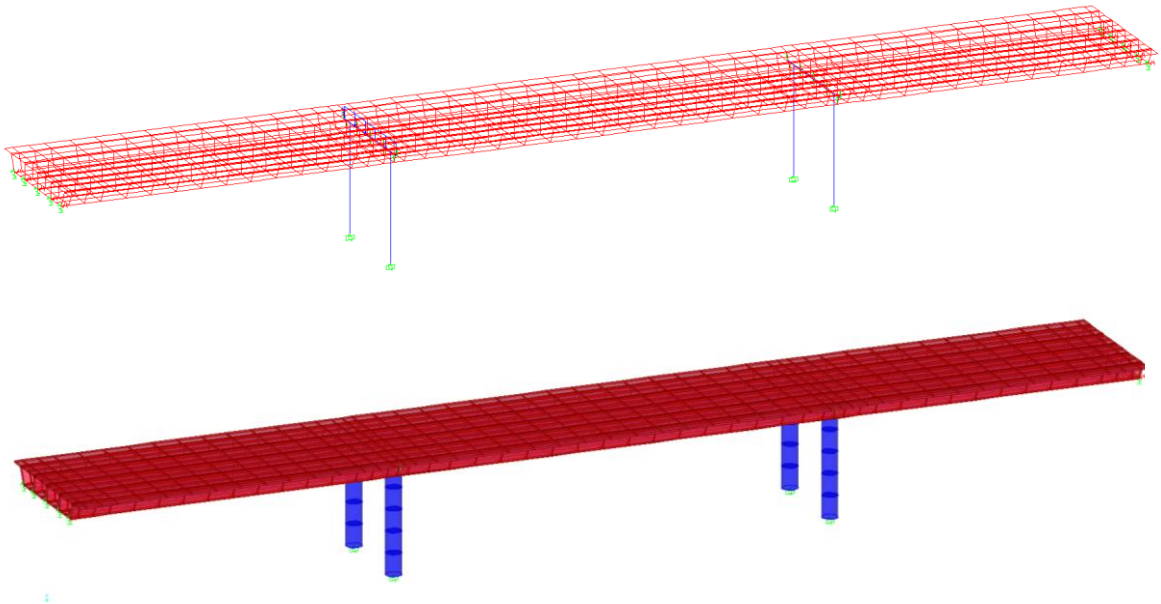

Figure 1- Original Model of Sample Bridge

1. Bridge Description

A 3-D finite element model is used to analyze the behavior of sub- and super- structure of multi cell box-girder bridge. As given in Figure 1, four cell box girder deck has the top slab width of 58’ 10”. The three- span continuous bridge is 412 ft long and the span lengths are 126 ft, 168 ft and 118 ft. The thicknesses of the top and bottom slabs are 9 1/8” and 8 1/4”, respectively. The depth of the box-girder is 6’ 9”. The connection between the super- and the sub- structures are through the integral cap beams with the same depth of the girders and 8 ft width. The original bridge superstructure is connected to two 6 ft diameter round columns through the moment resisting rigid connections. In the further analyses, the influence of the moment-free bearing configuration is also investigated as well. Note that the pile caps are not included in the model and the bottom ends of the columns are restrained as fixed in all six degree-of-freedoms.

The unconfined concrete strength is assumed to be 4000psi and the reinforcing steel is taken as Grade 60 with the ultimate stress capacity is 90 ksi. The prestressing tendons have the peak stress of 270ksi and their yield stress is 230ksi. The area of tendons in each section is 9in^2 and the initial prestressing force is set as 1824kips without the losses. The total loss in the prestressing force is assumed 20 ksi including the elastic shortening, creep, shrinkage and the steel relaxation stresses. The tendons are considered in parabolic geometry along the girders and all section moment-curvature calculations include the exact location of the tendons in the sections analyses. The reinforcing steel detail in the box-girders is given in Figure 2 where the transverse bars are also included in the moment-curvature analysis of the transverse sections.

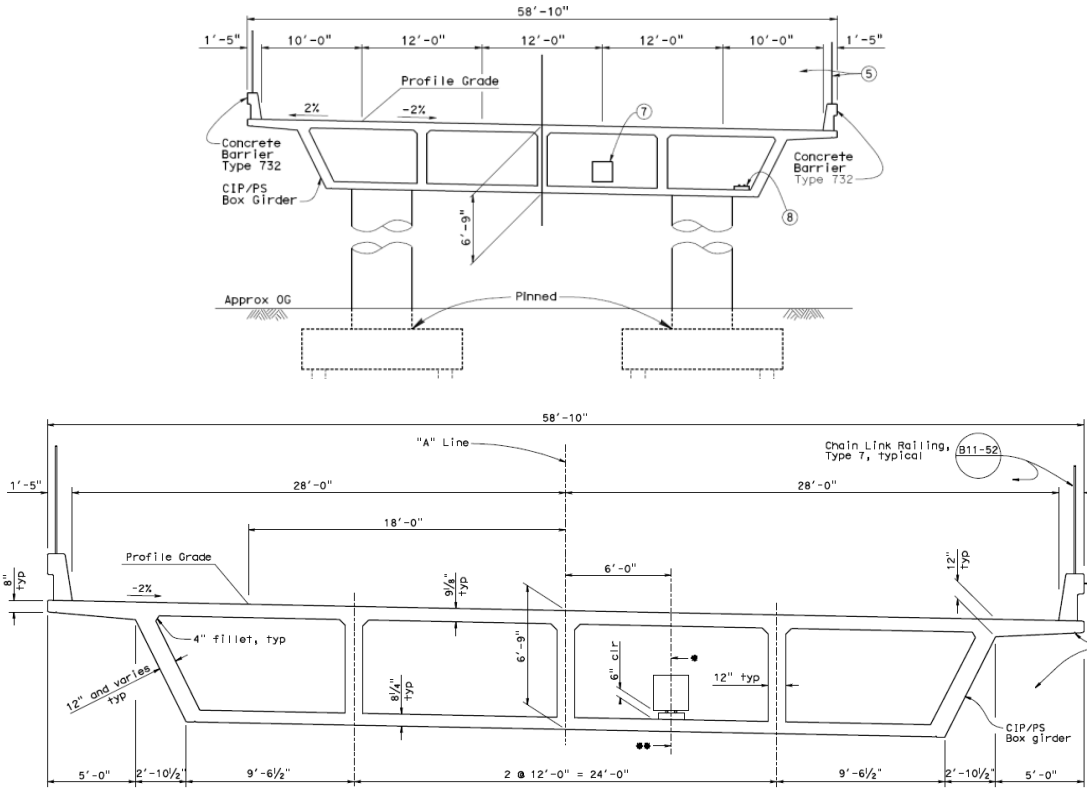

Figure 1- Typical Bridge Section and the Pier Columns with the Cap Beam

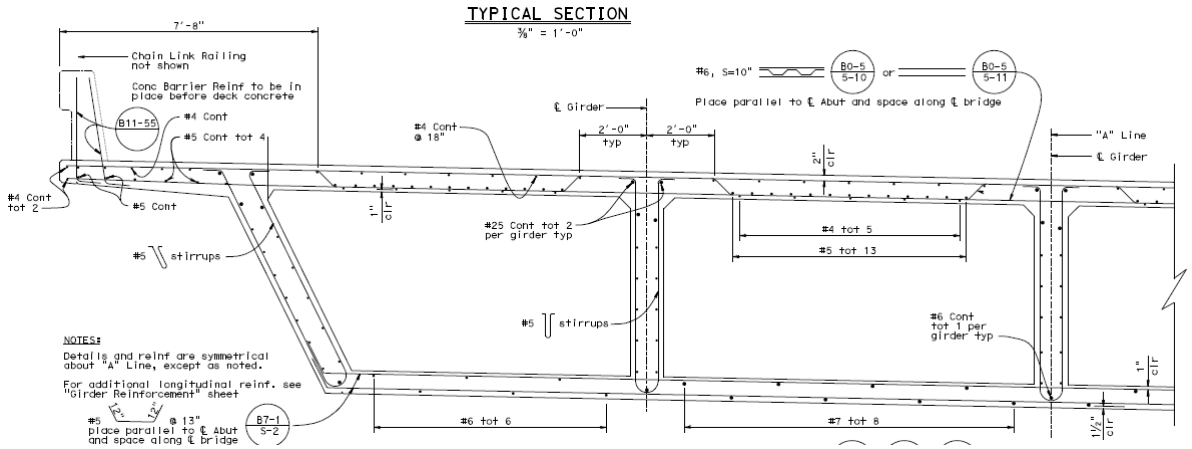

Figure 2- Reinforcing Steel Details of the Girders and the Top and Bottom Slabs

2. Analysis for Lateral Load: Model 1 with Rigid Cap-Column Connections

The lateral push-over analysis of the original model is straightforward using SAP2000. The plastic hinge definitions are applied at the bottom and top of the columns to capture the non-linear axial-flexure interaction. The plastic hinge definition is applied at the bottom surface of the integral cap beam as illustrated in Figure 3. The nonlinear pushover analysis tracks the plastic deformations at these locations.

The lateral pushover analysis is initiated with a nonlinear dead load, tendon jacking and live load analysis that provide the initial stresses in the elements. The dead load is calculated through the self-weight feature of SAP2000 and then the pre-stressing tendon jacking forces are applied to provide the initial condition of the bridge prior to an extreme event case. Note that the bridge is loaded by 20% of the HL93 load along two lanes to represent the regular traffic that may be on the bridge during an earthquake.

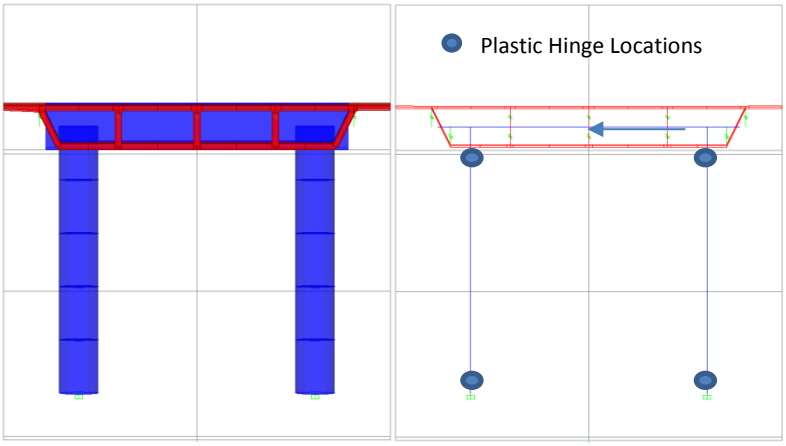

Figure 3- Model 1 Cross Sections with integral connection between cap beam and column

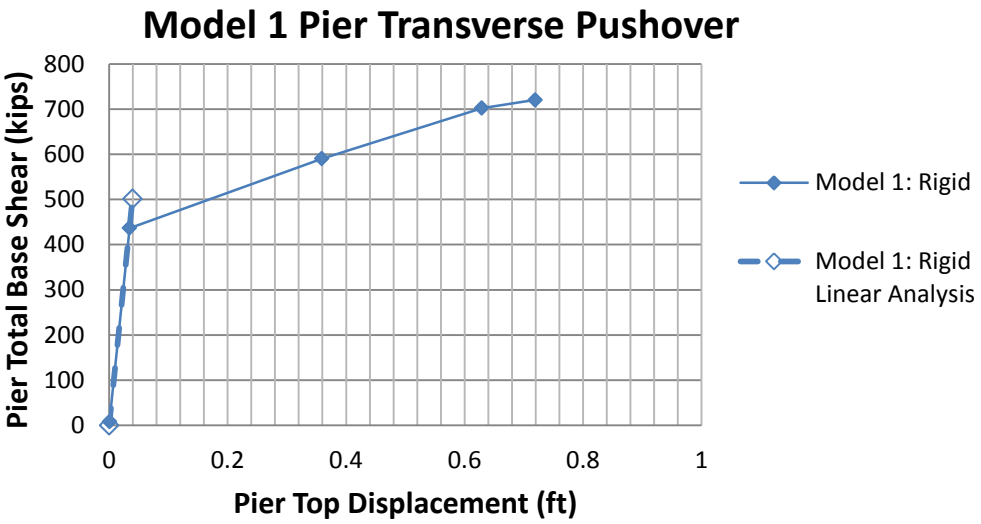

Figure 4- Model 1: Original Model Horizontal Pushover Curve

The plastic deformations are initialized at a total base shear of 437 kips. In Figure 4, the global response indicates a hardening behavior after plastic deformations has started at this 437 kip load level. At the last load step, where the total base shear on the pier is 720kips, the concrete compressive strain exceeds the ultimate limit and the section is crushed at bottom of the columns. Note that the transverse base shear capacity of the pier is also evaluated using a linear elastic analysis to compare with the non-linear analyses results. The bottom section of the pier reaches its ultimate flexure capacity at 501 kips. The linear analysis does not incorporate the load re-distribution during the plastic behavior of the sections and underestimates the entire capacity of the pier. The deformed shape at this final load step is illustrated in Figure 5. The sectional moment curvature response of the column is illustrated in Figure 6 where the extreme concrete fibers fail due to the strain exceeding the limit spalling strains and then the compression fibers in the confined concrete region reach the ultimate compressive strain limits.

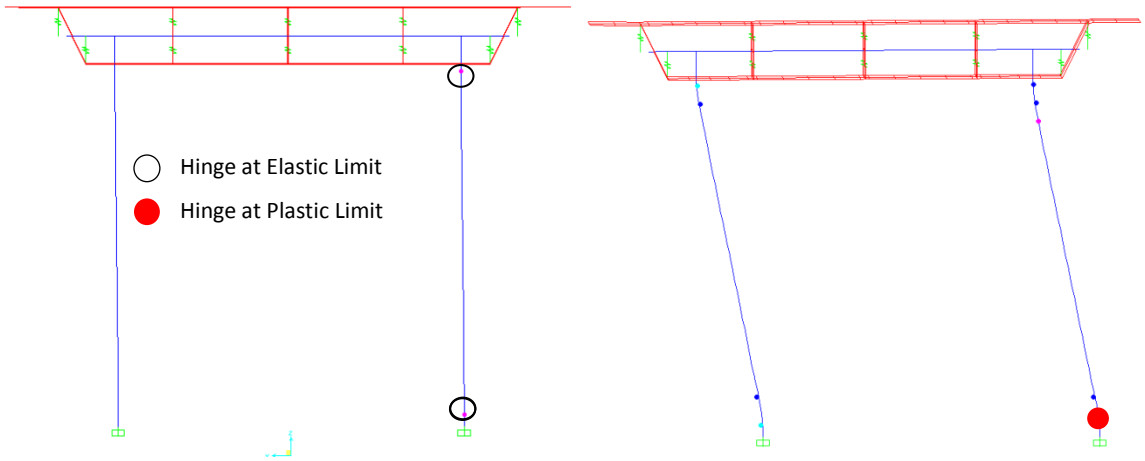

Figure 5- Model 1: (a) The first step where column top and bottom sections exceed elastic limits, (b) Failure due to concrete compressive strains exceeding crushing limit.

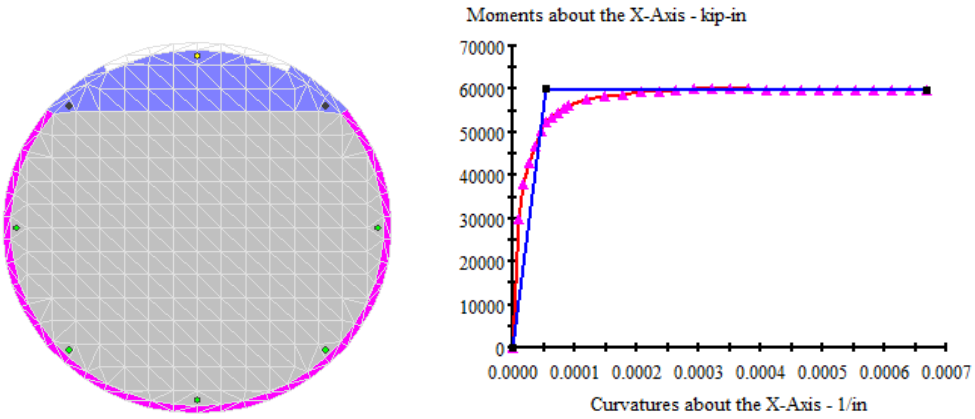

Figure 6- Column Section Behavior Showing Compressed Concrete Region in Dark Blue and Moment Curvature under the DL and 20% LL axial force.

3. Analysis for Lateral Load: Model 2 with Released Connections (Bearings)

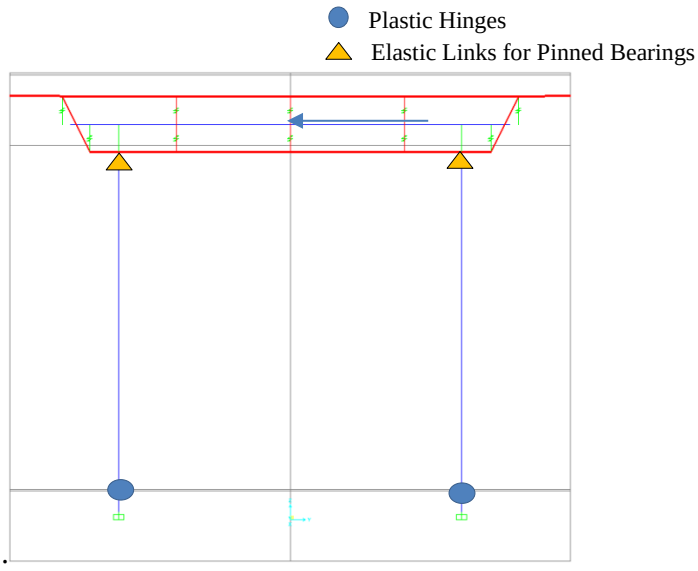

Figure 7- Model 2 Cross Sections with elastic links (pinned bearings) at the Pier

Model 1 is modified assuming that the cap beam is connected to the columns through bearings applied between the top of the column and the cap beam as illustrated in Figure 7. Elastic links are used to model the pads that serve to release the rotations at the top of the columns with the rotational stiffnesses of these bearings being set at zero. For the transverse and longitudinal translation, the elastic stiffness of the link is

infinitely large assuring the compatibility of the longitudinal and transverse displacements between the columns and the cap beam at the location of the bearings.

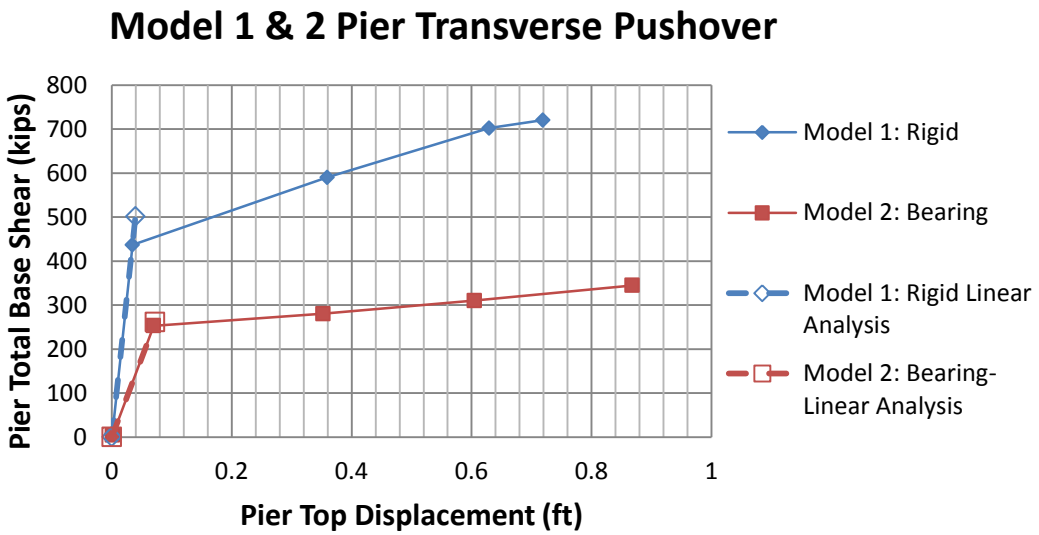

Figure 8- Transverse Pushover Analysis of the Pier with Bearings

Figure 8 compares the results of the push over analysis performed for Model 1 and Model 2. At the elastic limit, the total base shear capacity of the pier for Model 2 with a bearing connection is equal to 252 kips, which is significantly lower than the results of Model 1 with the rigid connection. The bearings provide a released flexure connection between the column and the cap beam and consequently, the bottom sections of the columns are subjected to significantly increased flexure demand when compared to the rigidly connected Model 1. Note that for the case with moment-released bearings, the level of indeterminacy is lower, thus linear analysis provides more accurate solutions than Model 1.

Figure 9 illustrates the fact that the released column top sections and the cap beam of the bridge with bearings do not contribute to structural resistance. At the final step, the bridge will fail when the load reaches 345 kips. At that load, the concrete section failure occurs when the concrete fibers in compression exceed the crushing limit while the reinforcing steel is in strain-hardening.

It is observed that the ultimate capacity for the Model 1 with the integral connection at 720 kips is slightly higher (by less than 5%) than two times the ultimate capacity of Model 2 with the bearing connections at 345 kips.

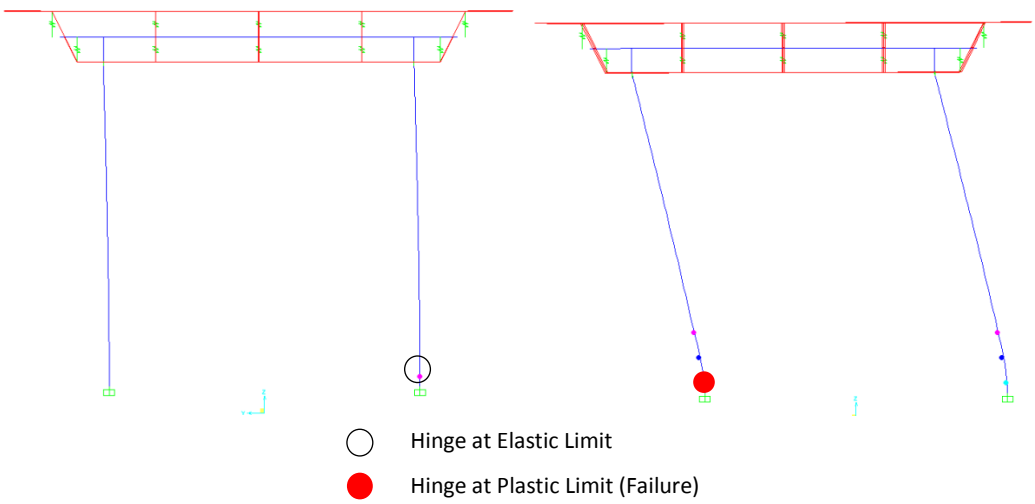

Figure 9- Model 2: (a) The first step where column bottom sections exceed their elastic limits, (b) Failure due to concrete compressive strains exceeding crushing limit.

4. Pushdown Analysis under Vertical Loads: Model 3 with Grillage

The nonlinear pushdown analysis under the effect of vertical load is not as straightforward as the lateral pushover analyses performed for Model 1 and Model 2. The shell element definitions for the reinforced concrete superstructure are not capable of representing the nonlinear behavior and interaction between the concrete and reinforcing steel fibers. Also, the pre-stressing tendons cannot be incorporated explicitly in the model. Instead, the original model represented the prestressing effects in terms of forces. Thus, the tendons physically do not exist in the model. However, with or without the physical tendon elements, the combined inelastic moment- curvature behavior cannot be represented using the original model.

Another commonly used option for representing the superstructure is the spline model which can simulate the inelastic behavior of this type of multi-cell prestressed concrete box girder superstructures. However, using a single beam element- type spline model will not be capable of capturing out-of-plane torsional effects whereas one of the goals in the model is to investigate the capacity of the superstructure in the presence of eccentric vertical loadings shifted to the curb which is further detailed.

Therefore, a new model is required where longitudinal/transverse flexure and torsional effects are represented accurately and the plastic hinge theory is applicable to capture inelastic behavior. The nonlinear behavior of the box-girder can be simulated by plastic hinge theory if the multi- cell box girder is modeled using a grillage where the transverse and longitudinal stiffnesses of the elements can be approximated. The flexural and torsional stiffnesses of the grillage elements are calculated through existing methodologies proven to capture box-girder behavior accurately [1, 2]. The grillage model for the superstructure can be connected to the beam column element representing the substructure such the entire bridge system is modeled as a space frame.

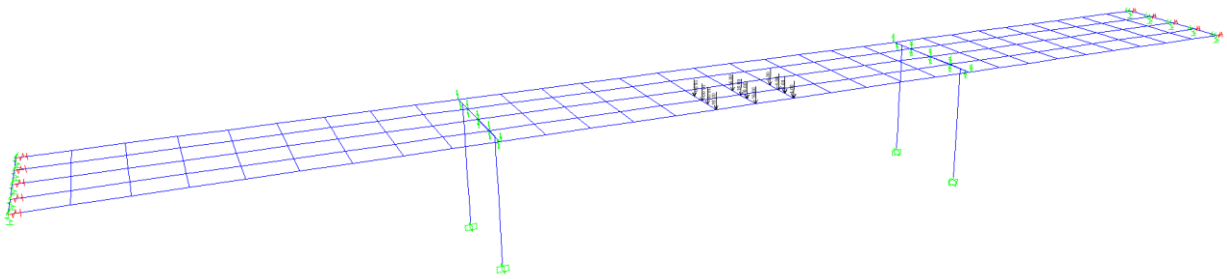

Figure 10- Model 3 Grillage/Space Frame Model with the HS20 Vehicle Loading

The longitudinal grillage elements represent the longitudinal stiffness of superstructure portions where each element carries the stiffness of the pre-stressed concrete web and the corresponding top/bottom slabs. For five webs, the model includes five longitudinal elements and the longitudinal stiffness I_L, is calculated from the geometry of each web portion and the proportional slab area.

The effective shear area of the transverse beams that distributes the loads in transverse and represents the cross section distortion (Figure 11) is evaluated by the closed form equation for an accurate approximation [1].

$$A_s = \frac{(t_t^3+t_b^3)}{S^2}\left[\frac{t_w^3\, S}{t_w^3\, S+d\,(t_t^3+t_b^3)}\right]\frac{E}{G} \quad \text{(Eq. 1)}$$

top slab thickness, t_t ; bottom slab thickness, t_b ; web thickness, t_w; depth between centerlines of the top and bottom slabs, d ; Spacing between adjacent webs of the cell, S.

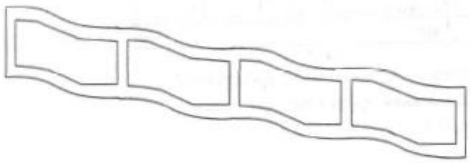

Figure 11- Cross Section Distortion Represented by I_t Stiffness

The transverse bending inertia has the closed form equation per unit length and the quantity is applied regarding the number of the transverse element of the grillage [1, 2].

$$I_t = \frac{d^2\, t_t\, t_b}{t_t+t_b} \quad \text{(Eq.2)}$$

Two formulations are available for the torsional stiffness of the longitudinal elements. The first formulation divides the total torsional constant J1 to be equally shared among the grillage longitudinal girders. The second formulation J2 is the other option which is calculated per unit length of the width. However, J1 is approximately twice the J2 stiffness. The non-linear analysis of the grillage is carried out only with the inelastic flexural effects wile torsional effect is assumed as elastic before the plastic hinge occurs. Initially, J2 stiffness is applied to the grillage girders so that the eccentric vertical forces are

carried by the flexure stiffness of the beams. This way, J2 is expected to provide more conservative flexural plastic capacity.

$$J1 = \frac{4A^2}{2b\sum ds/t} \quad J2 = \frac{2\,d^2\,t_t\,t_b}{t_t+t_b} \quad \text{(Eq.3)}$$

The plastic hinge definition for the grillage elements is based on the moment-curvature relationship of each web and corresponding slab portion. The pre-stressing strands and the conventional reinforcing steel are included in the section definitions. The SAP2000 program cannot incorporate the tendon pre-stressing effects in sections other than Caltrans' sections. However, the program allows the analyst to apply user-defined moment-curvature relationships at the plastic hinge definitions. Thus, the pre-stressed girders are evaluated outside the program and then their moment-curvature definition is assigned as user-defined. Xtract Software was used to obtain the moment-curvature relationships of the pre-stressed sections at each girder element along the bridge. Then, the plastic hinges are described in SAP2000 using the idealized bilinear moment-curvatures due to the SAP2000 program which only allows linear hardening/softening behavior within plastic region. Note that the Xtract bi-linearization technique is not always as accurate as the one given in Figure 12. Thus, a segmental regression analysis was carried out using available open-source codes [3] that provide the mathematically consistent idealized curves represented by one line for elastic and one line for the plastic region. Note that the average strength increase is 1.3 times the moment in elastic limit and provides significant capacity through hardening in the plastic region of the moment- curvature curves.

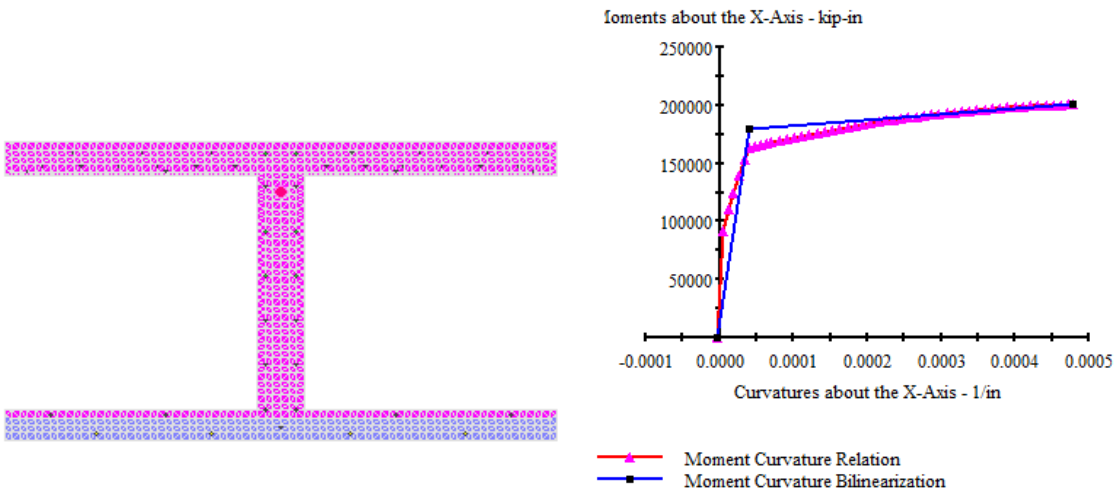

Figure 12- Negative Moment Curvature Section 126 where Failure is due to Rupture of the Tendons

As illustrated in Figure 13, two HS20 trucks with 4 ft distance are applied at the mid-span. The model is beam- type grillage where the transverse element locations are adjusted to make truck point loads coincide with the nodes. Note that the dead load is not incremented during the vertical push-down analysis.

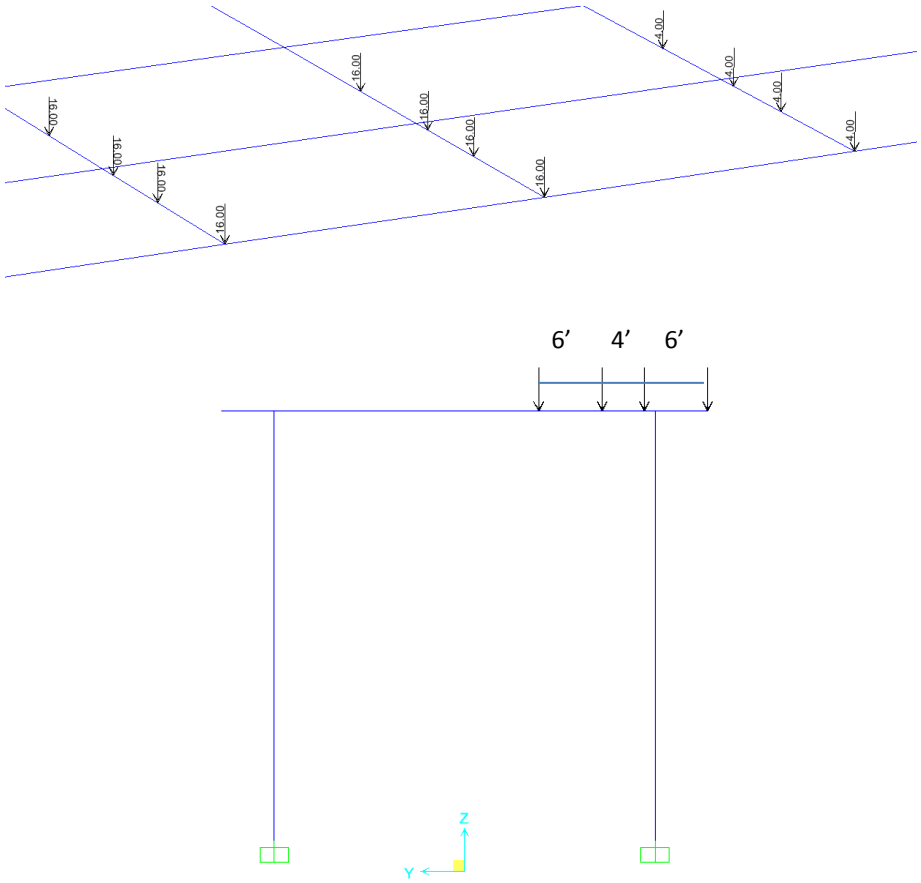

Figure 13- 2-Lane HS20 Truck Loading Locations Coinciding with the Grillage Mesh

The plastic hinge definitions of the program are applied at the critical location where the plastic deformations are expected at the connection regions and the point load locations as illustrated in Figure 14. The plastic hinge defintions provide the analyst the ability to track the elastic and plastic deformation levels. Note that for each end of the transverse elements, corresponding non-linear moment curvature curves of the section are assigned as well to represent the influence of top and bottom slabs of the box girders on the transverse stiffness.

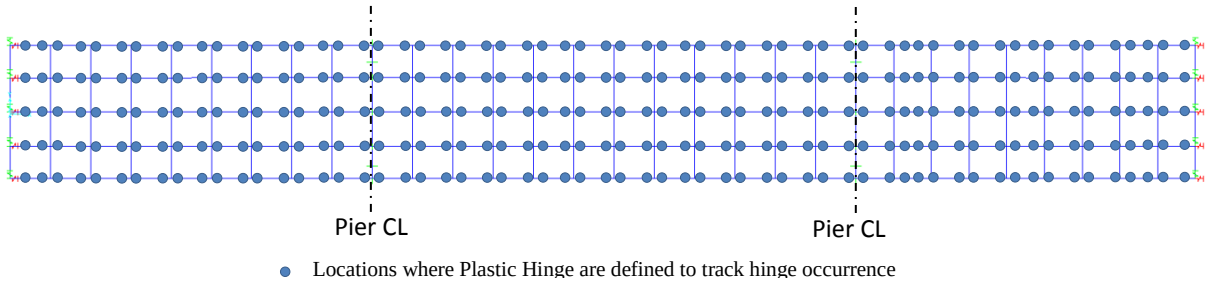

Figure 14- Plastic Hinge Locations at Pier Centerlines and the vehicle loads.

The vertical pushdown analysis results are presented in terms of the total vehicle axle load and the recorded displacement in the exterior girder at the midspan.The pushdown analysis is started after the dead load (DL) and the pre-stress (PS) loading are applied in a nonlinear analysis. Therefore, at the end of the initial DL+PS analysis, the pushdown curve starts at a vertical displacement equal to 0.12 ft at Step 0. The toal vertical force applied on the structure is then normalized by the total weight of two trucks, 144 kips and the load level is simply reported as a function of the Normalized Vertical Load (NVL) as given in Figure 15. The plastic strains are initiated at NVL=12.9 on the exterior girder support due to negative flexure and in both the interior and exterior girders due to positive flexure at midspan. Due to the eccentric vertical loads, the distortion behavior along the bridge section is well-simulated with appropriate shear stiffness calculated by the refered formulations. Note that the plastic hinges also occur in the transverse elements as the load steps are further increased. Figure 15 also includes the linear analysis solution for the vertical live load capacity of the superstructure where the midspan positive moment capacity is at NVL=18.0, and negative moment capacity occurs at NVL=18.6. Thus, the linear analysis results underestimates the load re-distribution among the girders once the plastic deformations occurs.

Maximum load capacity is at NVL= 24.1 when the total maximum vertical displacement of the midspan is 1.84 ft. Note that the recorded section failure is due to the extended pre-stress tendon fibers exceeding the ultimate strain limit of 0.035 in/in at the negative moment section as indicated in Figure 16 (b). A detailed deformed shape of half of the middle span is given in Figure 17 where the distortion in the bridge section is illustrated including the locations of plastic hinges occured at the peak load level.

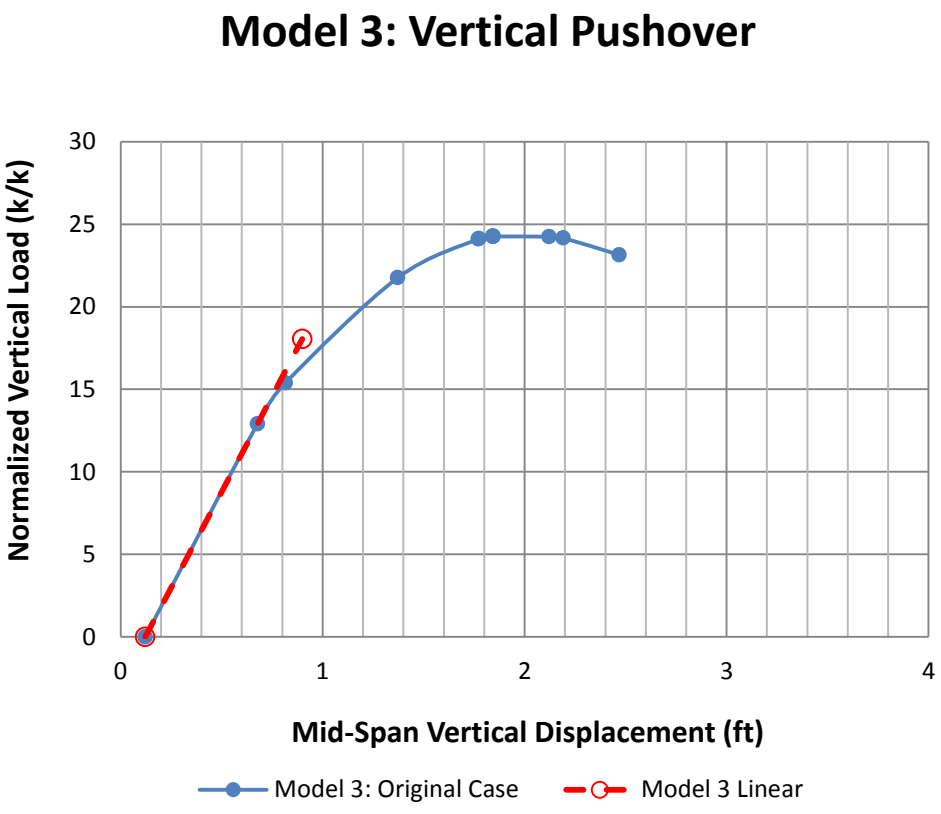

Figure 15- Vertical Pushover Analysis of the Original Model with No Deficiency.

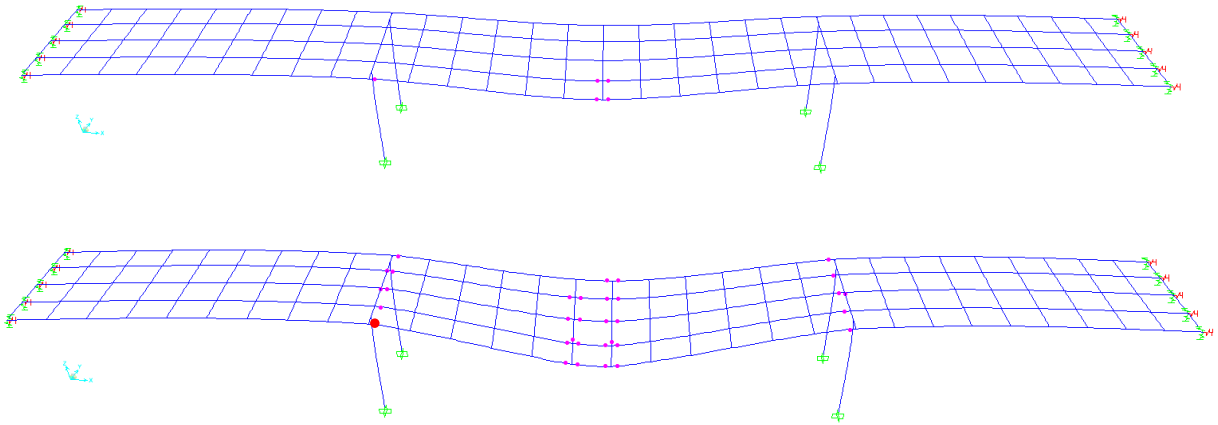

Figure 16- Model 3 (a) The first step where pre-stressed girder sections exceed elastic limits, (b) Failure due to the tendon stress reaching the ultimate strain.

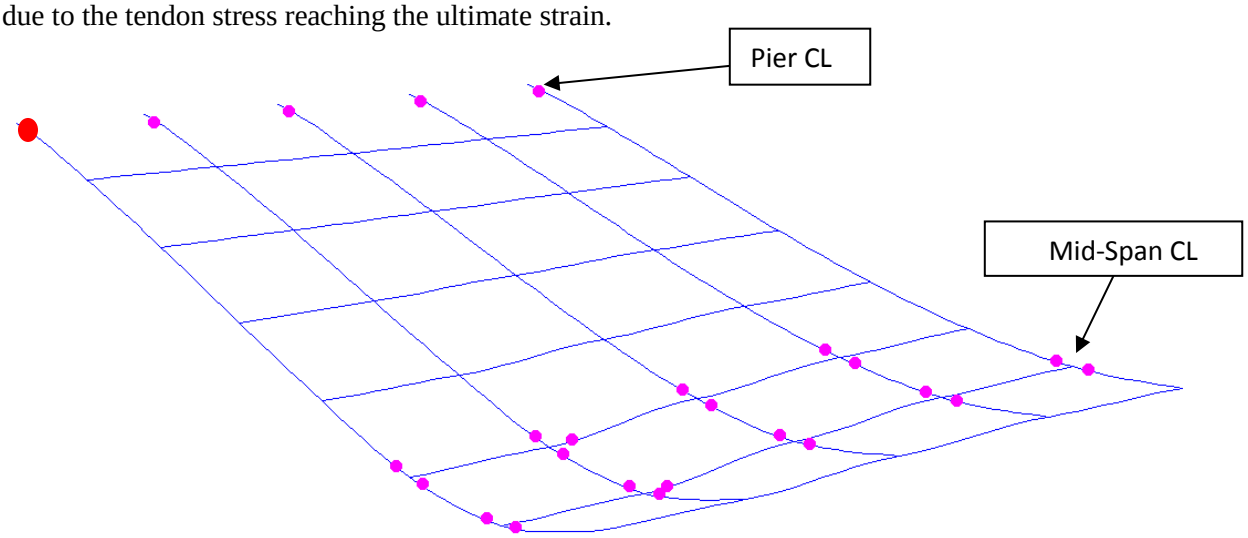

Figure 17- Model 3 Distortion at the Mid-span Due to the Eccentric Vehicle Loading.

5. Vertical Load Analysis with Damage Scenario I: Model 4 Column Removal

The push-down analysis is repeated in Model 4 where one of the piers is removed from the system to study the capacity of the system to carry some load following major damage to one of the columns. This first damage scenario as illustrated in Figure 18 could represent a situation where one of the column is hit by a truck, ship or debris carried by a flood or when one column foundation is damaged to a major scour or if one of the columns has been exposed to major deterioration or construction errors. Note that the initial plastic hinge definitions given in Figure 18 can be increased near the undamaged pier and, again, around the vehicle axle loads. Within the scope of the damage bridge scenarios undertaken in this study, the dynamic impact of the element loss is not included in the static pushdown analyses. The objective is to study the ability of a system that has sustained some major damage to continue to carry load and not the response of the bridge to the dynamic impact.

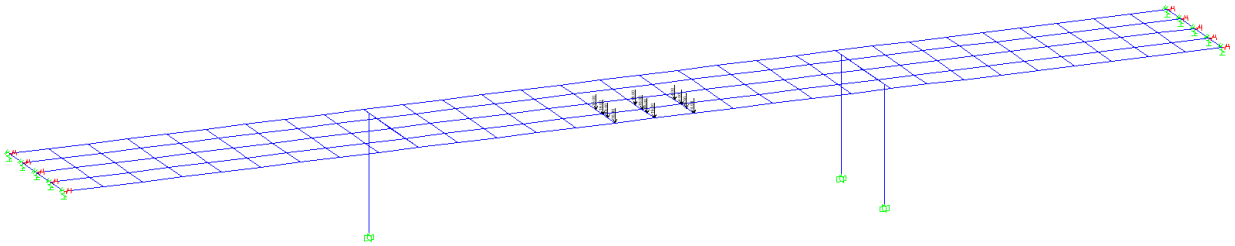

Figure 18- Damage Scenario I with the Removed Pier Column

The analyses of Model 4 is carried out in two scenarios. The first scenario followed is given in Model 4-a where the columns sections are assumed to behave within linear elastic limits. Due to the loss of one pier column, the amount of flexure demand on the undamaged column of the same pier is expected to be extreme, so that the failure modes are probable in this column section. In the first scenario, the focus is directly on the load distribution on the superstructure, thus the column sections are assumed to behave in elastic manner to investigate the effects of load distribution only in the superstructure. Figure 19 illustrates the failed girder section plastic hinges due to excessive negative moment demand at the undamaged pier location. Note that the plastic hinges also occur on the cap beam; however, these sections, which are already yielded, do not reach their failure limits before the girder sections in this analysis.

The second scenario, Model 4-b, is a more realistic approach that represents the nonlinear material behavior in both super- and sub- structures. In this case, the plastic hinges are also defined in the column sections to monitor the plastic behavior of the sub-structure as well. Note that the behavior of Model 4-b with the column loss is expected to be governed by the plastic deformations and probable failure modes in the column and/or the cantilevered cap beam sections. Figure 20(a) illustrates the deformed shape of the bridge at the initial step where the plastic hinges are already initialized in the cap beam and the column when the structure with the column loss is subjected to the dead load and pretressing force effects (DL+PS). Figure 20(b) illustrates the plastic hinge propagation when the column section is failed due to the excessive compressive strains in the conrete. Then, the section loses its entire flexure stiffness, starts unloading and behaves as a flexure hinge after this point. The pushdown analysis is continued after the load redistribution due the the column flexural failure and the vertical vehicle loads are increased until the critical girder section failure at the midspan of Span 2 as given in Figure 20 (c).

The numerical results of the vertical pushdown analyses on the Models 4-a and 4-b are compared to the original case (Model 3) in Figure 21. Regarding the results from Model 4-a where the sub-structure columns is in elastic manner, the prestressed girders are significantly redundant when one of the piers in the structure is subjected to a column loss. Model 4-a experienced the girder failure at the negative moment section of the exterior girder at the peak level of the normalized vertical load, NVL = 23.8. Recall that this value is slightly smaller than the original case, Model 3 with NVL=24.1.

The column plastic hinge reached its ultimate plastic deformations capacity at NVL=11.Note that the plastic hinge is already initiated due to the re-distribution of dead and prestressing loads. The vertical pushdown is resumed while the failed column section is unloaded until the critical girder section at the

midspan is failed due to the excessive plastic strains in the pre-stress tendon in the exterior girder (NVL=19.0).

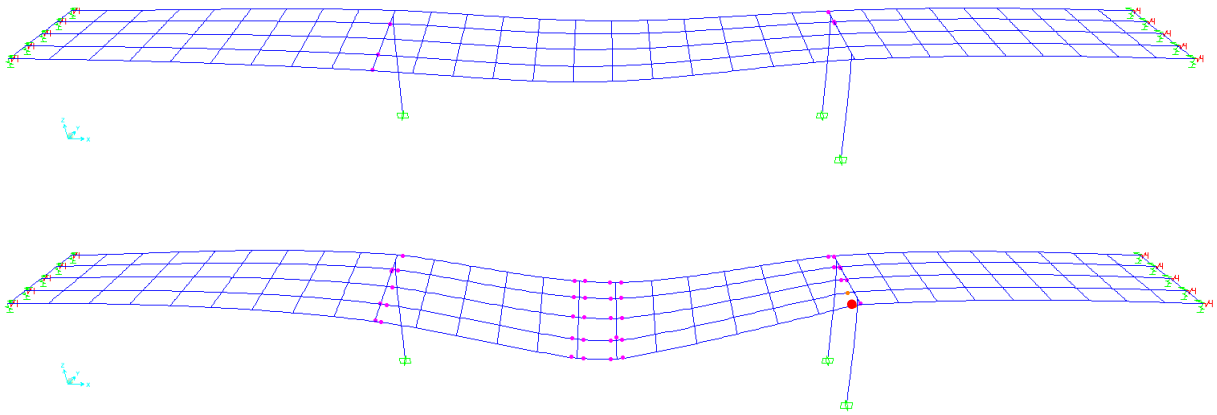

Figure 19- Model 4-a (a) The first step where the cap beam sections exceed elastic limits, (b) Failure due to the tendon stress reaching the ultimate strain at the negative moment section along the centerline of undamaged pier.

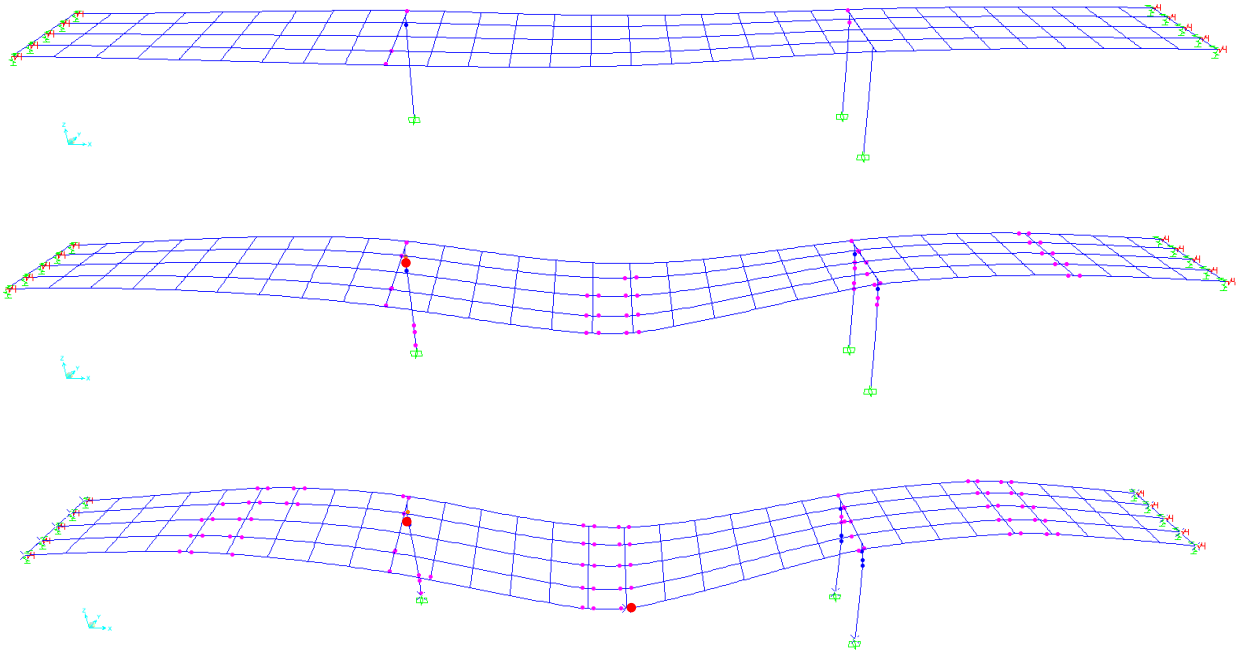

Figure 20- Model 4-b (a) The first step where the column sections exceed elastic limits, (b) Failure in the top column sections, the section immediately starts unloading after this point. (c) First failed pre-stressed girder failure

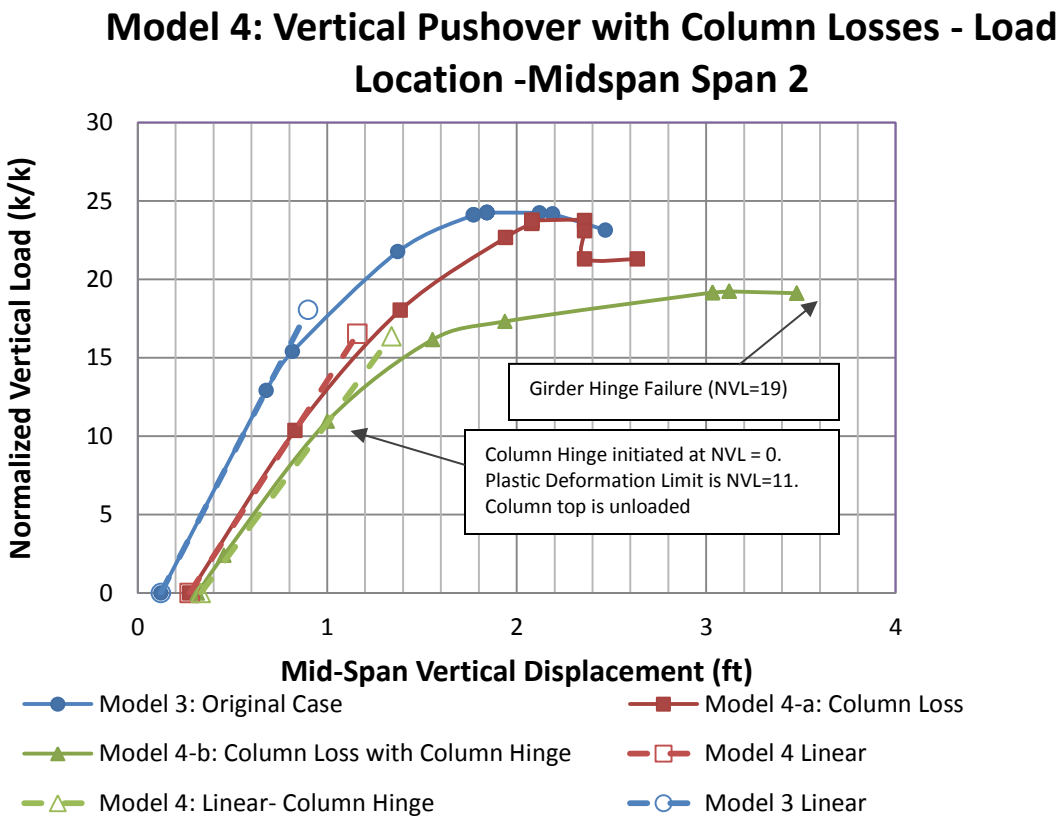

Figure 21- The Effects of Column Removal on the Vertical Pushdown Analyses of Pre-stressed Girders.

The linear analysis solution for Model 4 cases are also included in Figure 21. The linear analysis in Model 4-a can not provide a sufficient represetation of the load re-distribution once the initial plastic hinges occur and underestimates the live load capacity at NVL=16.5. In the presence of plasticity in the columns, the linear analysis is performed on the system where the column top seciton is released for both moment directions. The linear solution indicates that the positive moment capacity at the midspan and the negative moment capacity at the support are reached at NVL=16.4 and NVL=16.8, respectively.The linear analysis solution for Model 4-c provides more accurate results when the column failure is also modeled.

Once the influence of the plasticity on the un-dameged colums is detected as significant, an additional model case (Model 4-c) is introduced as an alternative case to check to evaluate the effect of the truck location on the failure mode. In Model 4-c, the two HL93 trucks are located over the damaged pier. As illustrated in Figure 22, the vertical load capacity of the system slightly different than each other. However the cricial member locations are not the same. The failure occurs on the girder plastic hinge near the support location due to the positive moment causing excessive compressive stress in the concrete. This failure mode is not similar to the ductile tendon failure at the midspan where the vehicles are loacated in Model 4-b.

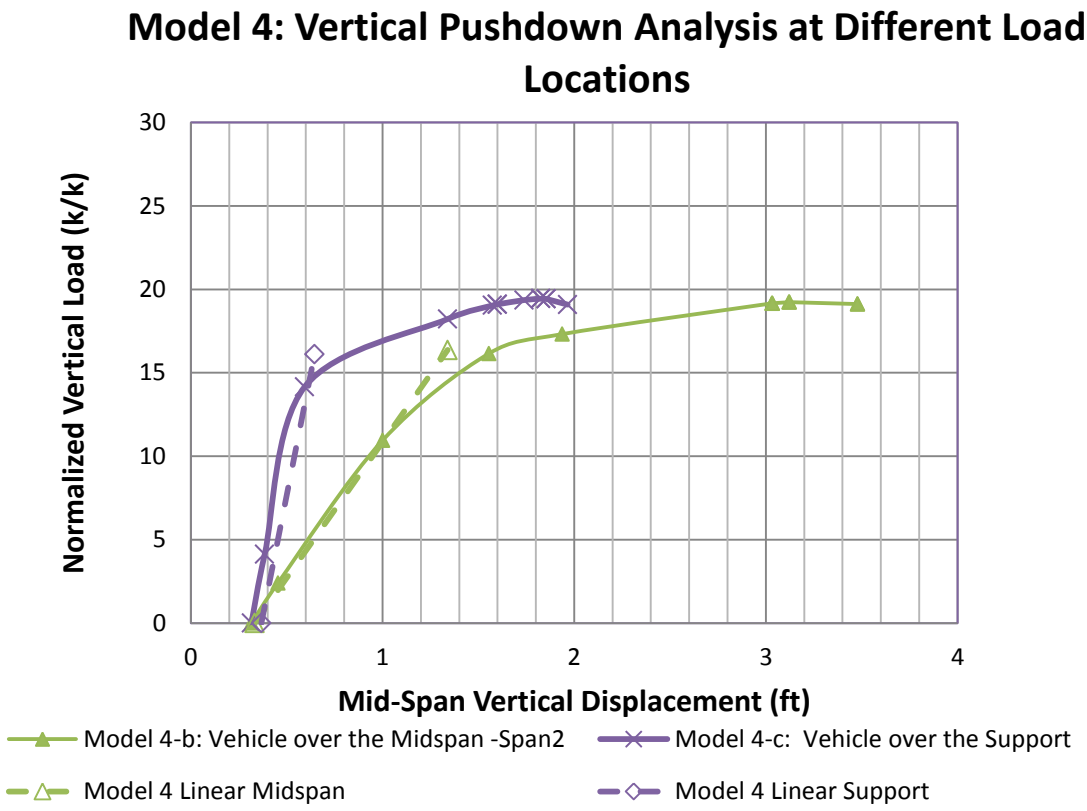

Figure 22- The Effects of Vehicle location on the Vertical Pushdown Analyses of Pre-stressed Girders.

6. Vertical Load Analysis with Damage Scenario II: Model 5 Web Removal

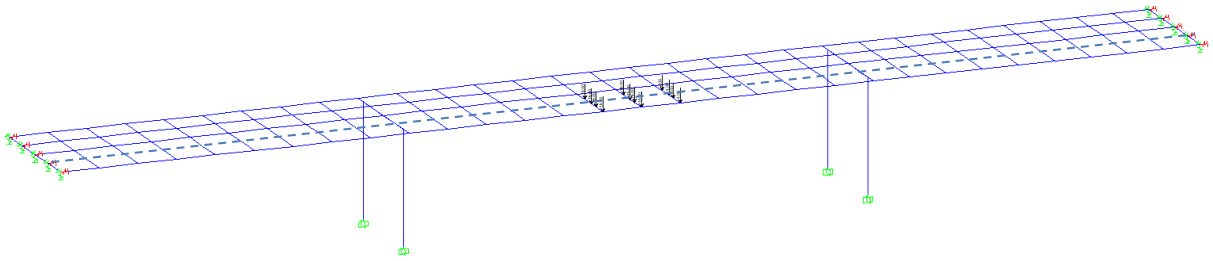

Figure 23- Damage Scenario II with the Removed Grillage Girder

The second damage scenario considered is the failure in the pre-stressing tendons in one of the webs. The case is represented by setting the flexural stiffnesses theoretically as zero along the length of the bridge. The second girder in the grillage model is selected as the failed girder to simulate a worst case scenario because the maximum demand in the originally intact system is expected on this girder due to the position of the two HS20 trucks.

Note that a significant load demand is expected on the transverse elements where multiple axle wheel loads are applied. When the damaged girder is removed, the transverse elements are expected to fail and both flexure hinge mechanisms are expected to occur on these elements. To model such effect accurately, additional releases are provided at the transverse member element ends.

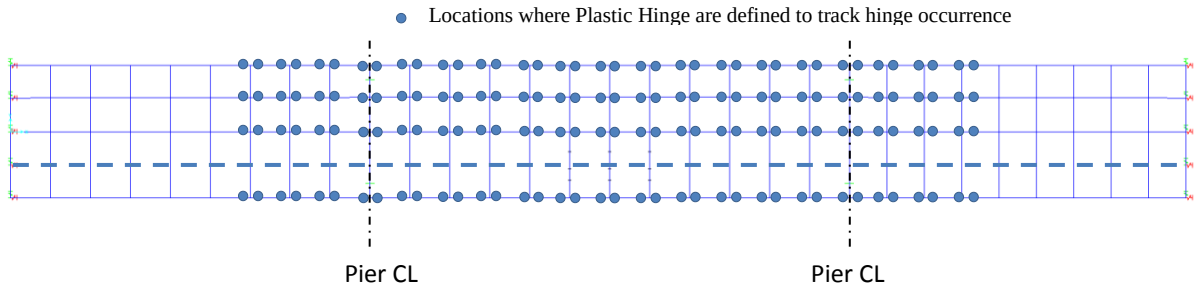

Figure 24- Plastic Hinge Locations at Pier Centerlines and the vehicle loads.

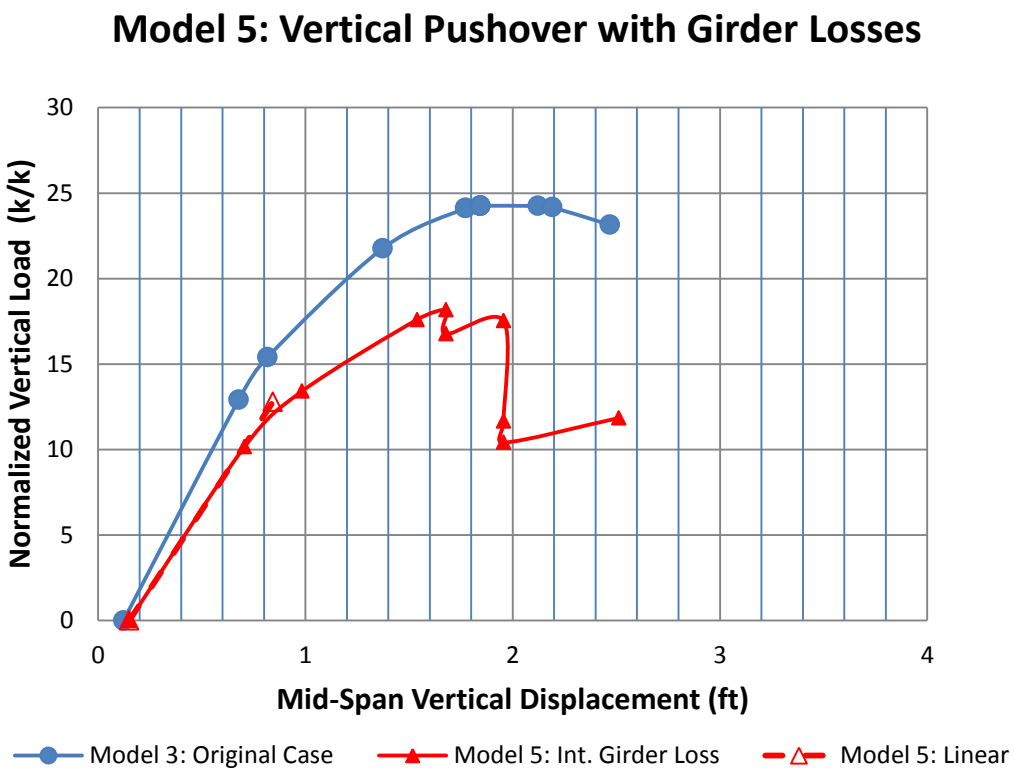

Figure 25- Vertical Pushdown Analysis of the Bridge with the Damage Scenario II, Girder Loss.

Due to the interior girder loss, the exterior girder becomes the most critical component when the structure is subjected to the eccentric vehicle load. The initial plastic hinges occurred at the pier and the midspan sections of the the exterior girder at the vertical load level, NVL = 10.2. As the vertical loads are increased, the flexure hinges are also observed at the mid points of the transverse elements where the points loads are applied. Finally, the pier section of the exterior girder reaches the flexure capacity as the

tendon exceeds the strain limit at the failure, NVL= 18.2 as given in Figure 25. Note that the linear analysis solution (NVL=12.8) is not accurate due to the load re-distribution after plastic hinge occurrence. The plastic hinge propagation is illustrated in Figure 26.

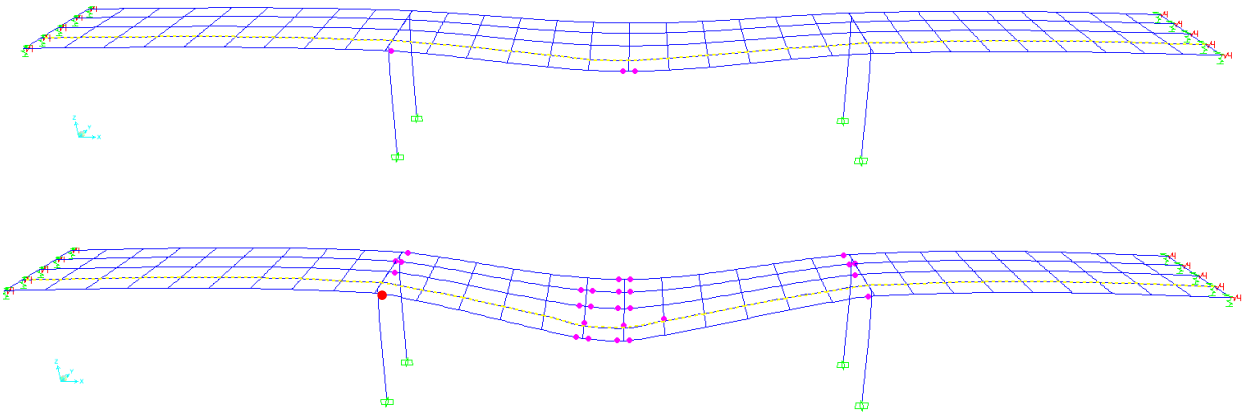

Figure 22- Model 5: (a) The First Step where the Exterior Girders Exceeded Elastic Limit (NVL=10.1), (b) the Plastic Hinge Failure at the Negative Moment Section of the Exterior Girder (NVL =18.2).

7. Redundancy Analysis and Comparisons

Table 1 summarizes the redundancy ratios for the different models. According to NCHRP 406, a redundancy ratio for the originally intact bridge subjected to overloading should produce a redudancy ratio LF_u/LF_1 greater than 1.3 to be considered suffciently redundant. Damaged bridges should give LF_d/LF_1 ratio of 0.50 or higher.

The redundancy ratios compare the maximum capacity of the system to that of the first member to fail. According to linear elastic pushover analysis of Model 1, the lateral force P_1 is 501kips when the bottom section of the pier reaches its ultimate flexure capacity. According to linear "pushdown" analysis of Model 3, if two trucks are loaded in the middle span, the first member fails in positive bending when the weight of these trucks is incremented by a factor at LF_1=18.0. The results of Model 1 through 3 in Table 1 show that this bridge provides good levels of redundancy for the ultimate limit state due to either vertical or lateral overloading of the originally intact bridge. The results of Model 4-a, -b, -c and Model 5 also show higher redundancy ratio than the minimum redundancy value of 0.50 for damaged scenarios. Therefore, this bridge satisfies all the redundancy criteria provided in NCHRP 406.

Table 1 Summary table for the redundancy ratio of the prestressed box-girder bridge

Analysis Case Model	P_u/P_1	LF_u/LF_1	LF_d/LF_1
Model 1	1.44	---	---
Model 2	1.37	---	---
Model 3	---	1.34	---
Model 4-a	---	---	1.32
Model 4-b	---	---	1.06
Model 4-c	---	---	1.06
Model 5	---	---	1.01

CONCLUSIONS

The system redundancy of a sample multicell prestrssed concrete box-girder bridge was evaluated through a set of non-linear static analyses accounting for the nonlinear behavior of the pier columns and the pre-stressed girder sections. The system behavior of the system under the effect of lateral load was evaluated for two cases: (1) Model 1 with the box-girder superstructure connected to the substructure through rigid integral connections between the capbeams and the columns; (2) Model 2 with the box-girder superstructure supported on bearings where the theoretical flexural stiffness was zero. The horizontal pushover analyses indicated that the horizontal load capacity of the system with pinned piers is reduced by 53% when compared to the performance of the system with integral column –cap beam connection. This reduction is consistent with currently used simplified plastic analysis models that consider the pier as a frame with either fixed-fixed columns simulating the behavior of the system with integral connection as compared to fixed-pinned columns which simulate the behavior of the system with bearings.

The pre-stressed multicell box girder bridge system redundancy was evaluated by analyzing the effects of two damage scenarios. In the first damage scenario the structure is assuemd to have experienced the loss of a pier column while the second scenario simulated the loss of a pre-stressed girder. The vertical pushdown analysis indicated that the eccentrically loaded bridge in its original undamaged condition had a total capacity capable of carrying up to 23.9 times the weight of two HS-20 vehicles located side-by-side between the exterior and the second interior girders on top of the dead load and the pre-stressing force effects. For the damaged scenario simulating the loss of one column, the remaining un-damaged column is subjected to significant flexure demand at the top section. The undamged column's flexure capacity rstarted its plastification at when the vertial load reached 11 times the weight of two HS-20 design vehicles applied at the midspan. However, due to girder load distribution the ultimate capcity was

not affected as severly as the column and the ultimate capacity of the system took place when the load reached 21 times the total vehicle loads.

The linear analysis solutions for the superstructure through five models are generally not sufficient to represent the load re-distribution among the prestressed girders. The linear solution underestimates the vertical and horizontal load capacity of super- and sub-structures due to the higher level of indeterminacy.

The damage scenario simulating the loss of a girder demonstrated that there was significant amount of redundancy in the system and large additional load distribution. The loss of a prestressed girder, reduces the capacity of the system by 76% compared to the original intact case. Due to the loads's eccentric location, the exterior girder away from the load and the first interior girder on the other side did not contribute significantly to the original load capacity of the intact system; therefore they are able to help carry additional load when the girder below the load is removed.

REFERENCES

[1] Zokaie T, Osterkamp TA, Imbsen RA. (1991) Distribution of Wheel loads on Highway Bridges. Final Report, NCHRP project 12-26; Transportation Research Board, The National Academies, 1991.

[2] Hambly EC. (1991) Bridge Deck Behavior. London: Chapman and Hall, Ltd;

[3] Muggeo V. (2008) Segmented: an R package to fit regression models with broken-line relationships. R News, 8, 1: 20-25.